Original Article

Idiopathic pulmonary fibrosis disease progression: a dynamic quantitative chest computed tomography follow-up analysis

Haishuang Sun[1,2,3], Min Liu[3,4], Han Kang[5], Xiaoyan Yang[2], Peiyao Zhang[4], Rongguo Zhang[5], Huaping Dai[2,3], Chen Wang[1,2,3]

[1]Department of Respiratory Medicine, The First Hospital of Jilin University, Changchun, China; [2]National Center for Respiratory Medicine, National Clinical Research Center for Respiratory Diseases, Institute of Respiratory Medicine, Chinese Academy of Medical Sciences, Department of Pulmonary and Critical Care Medicine, Center of Respiratory Medicine, China-Japan Friendship Hospital, Beijing, China; [3]Chinese Academy of Medical Sciences and Peking Union Medical College, Beijing, China; [4]Department of Radiology, China-Japan Friendship Hospital, Beijing, China; [5]Institute of Advanced Research, Infervision Medical Technology Co., Ltd., Beijing, China

Contributions: (I) Conception and design: M Liu, H Dai, C Wang; (II) Administrative support: M Liu, H Dai; (III) Provision of study materials or patients: H Sun, X Yang, P Zhang, H Dai; (IV) Collection and assembly of data: H Sun, M Liu, X Yang; (V) Data analysis and interpretation: H Sun, M Liu, X Yang, H Kang, R Zhang; (VI) Manuscript writing: All authors; (VII) Final approval of manuscript: All authors.

Correspondence to: Min Liu. Department of Radiology, China-Japan Friendship Hospital, Yinghua Dong Street, Hepingli, Chaoyang District, Beijing 100029, China. Email: mikie0763@126.com; Huaping Dai. Department of Pulmonary and Critical Care Medicine, China-Japan Friendship Hospital, Yinghua Dong Street, Hepingli, Chaoyang District, Beijing 100029, China. Email: daihuaping@ccmu.edu.cn; Chen Wang. Department of Pulmonary and Critical Care Medicine, China-Japan Friendship Hospital, Yinghua Dong Street, Hepingli, Chaoyang District, Beijing 100029, China. Email: cyh-birm@263.net.

Background: To clarify whether dynamic quantification of variables derived from chest high-resolution computed tomography (HRCT) can assess the progression of idiopathic pulmonary fibrosis (IPF).

Methods: Patients with IPF who underwent serial computed tomography (CT) imaging were retrospectively enrolled. Several structural abnormalities seen on HRCT in IPF were segmented and quantified. Patients were divided into 2 groups according to their pulmonary function test (PFT) results: those with disease stabilization and those with disease progression, and differences between the groups were analyzed.

Results: There were no statistically significant differences between the 2 patient groups for the following parameters: baseline PFTs, total lesion extent, lesion extent at different sites in the lungs, and pulmonary vessel-related parameters (with P values ranging from 0.057 to 0.894). Median changes in total lung volume, total lesion volume, and total lesion ratio were significantly higher in patients with worsening disease compared with those with stable disease (P<0.001). There was a significant increase in total lesion volume of 214.73 mL [interquartile range (IQR), 68.26 to 501.46 mL] compared with 3.67 mL (IQR, −71.70 to 85.33 mL) in the disease progression group compared with the disease stability group (P=0.001). The decline in pulmonary vessel volume and number of pulmonary vessel branches was more pronounced in the group with functional worsening compared with the group with functional stability. Moreover, changes in lesion volume ratio were negatively correlated with changes in diffusing capacity of the lungs for carbon monoxide (DLco) during follow-up (R=−0.57, P<0.001), and changes in pulmonary vessel-related parameters demonstrated positive correlation with DLco (with R ranging from 0.27 to 0.53, P<0.001) and forced vital capacity (FVC) (with R ranging from 0.44 to 0.61, P<0.001).

Conclusions: Changes in CT-related parameters during follow-up may have better predictive performance compared with baseline imaging parameters and PFTs for disease progression in IPF.

Keywords: Idiopathic pulmonary fibrosis (IPF); quantitative computed tomography (CT); high-resolution computed tomography (HRCT); progression

Submitted Aug 11, 2022. Accepted for publication Dec 09, 2022. Published online Jan 09, 2023.
doi: 10.21037/qims-22-843
View this article at: https://dx.doi.org/10.21037/qims-22-843

Introduction

Idiopathic pulmonary fibrosis (IPF) is a rare and irreversible interstitial lung disease (ILD) with a median survival time of only 2 to 5 years after diagnosis (1). The evaluation of disease progression in patients with IPF is crucial, as it influences treatment decisions when assessing response to therapy. Currently, the accepted gold standard for defining clinical deterioration in patients with IPF is a decline in forced vital capacity (FVC) (2,3). By contrast, the significance of marginal change (5–10%) is unclear, and sensitivity is low because of its variability (4). Moreover, pulmonary function tests (PFTs) only reflect overall lung function and cannot be performed with patients with severe IPF. Several prior studies have demonstrated that semiquantitative visual assessment of fibrosis extent using high-resolution computed tomography (HRCT) predicts prognosis of IPF (5-7). However, this method is subjective and susceptible to interobserver variability (8). Recently, computer-assisted quantitative CT (QCT) has attracted the attention of researchers, because it has been shown to be more accurate than visual scoring (6). Multiple studies have shown that the extent of lesions on CT correlates with prognosis in IPF (6,9), whereby the term 'lesions' encompasses the 4 typical features of IPF seen on CT (honeycombing, reticular pattern, ground glass opacity, and traction bronchiectasis). However, most of these studies focused on lesion extent at baseline. Additionally, pulmonary vessel volume based on QCT has been reported to be associated with disease severity and prognosis in IPF (10). The current study aims to explore changes in lesion extent ratios at different sites in the lungs as well as changes in pulmonary vessel-related parameters on CT between the 2 patient groups based on changes in their PFTs. The following article is presented in accordance with the STROBE reporting checklist (available at https://qims.amegroups.com/article/view/10.21037/qims-22-843/rc).

Methods

Study cohort and design

All patients were included retrospectively if they were diagnosed with IPF at the Department of Pulmonary and Critical Care Medicine, China-Japan Friendship Hospital, by a multidisciplinary team between October 2016 and May 2021, and if they were followed-up up until December 2021. Diagnoses were based on the 2011 American Thoracic Society, European Respiratory Society, Japanese Respiratory Society, and Latin American Thoracic Association (ATS/ERS/JRS/ALAT) criteria. The study was conducted in accordance with the Declaration of Helsinki (as revised in 2013). The study was approved by the Ethics Board of the China-Japan Friendship Hospital (No. 2017-25), and individual consent for this retrospective analysis was waived. The inclusion criteria were as follows: (I) patients who underwent at least 2 thin-section (high-resolution) CT chest scans; and (II) diagnosis of PFTs occurred within 1 week of completing both HRCTs. The exclusion criteria were as follows: (I) comorbid pulmonary diseases such as malignant tumors and lung infections; (II) heart failure; and (III) significant respiratory motion artifacts. The flowchart was shown in *Figure 1*.

CT protocol

All cases were scanned from the lung apex to the lung base in a supine position with full inspiration using a multislice spiral CT scanner (Lightspeed VCT/64, GE Healthcare, Chicago, IL, USA; Toshiba Aquilion ONE TSX-301C/320, Toshiba, Tokyo, Japan; Philips iCT/256, Philips, Amsterdam, The Netherlands; and Siemens FLASH Dual Source CT, Siemens, Erlangen, Germany). The acquisition and reconstruction parameters of HRCT scans were as follows: tube voltage of 100–120 kV, tube current of 100–300 mAs, section thickness setting of 0.625 to 1 mm, table speed of 39.37 mm/s, gantry rotation time of 0.8 s, and reconstruction increment of 1 mm.

Lesion segmentation and quantification

A deep learning approach (InferReadTM CT Lung, version R3.12.3; Infervision Medical Technology Co., Ltd., Beijing, China) was used for lung segmentation and calibration and was performed by 2 radiologists with 9 and 15 years of clinical experience. The lungs were trisected vertically and divided in the axial plane into right upper lung, right

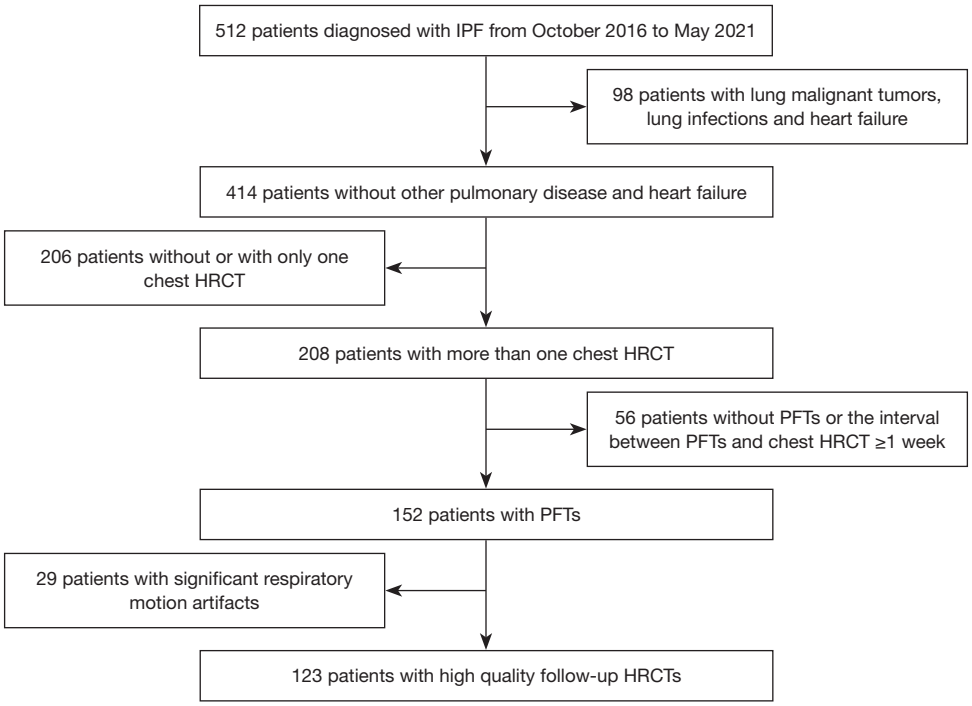

Figure 1 Study design flow chart. IPF, idiopathic pulmonary fibrosis; PFT, pulmonary function test; HRCT, high-resolution computed tomography.

middle lung, right lower lung, left upper lung, left middle lung, and left lower lung (i.e., not by anatomical lung lobes). The 4 typical imaging features of IPF on chest HRCT (honeycombing, reticular pattern, ground glass opacity, and traction bronchiectasis) were manually segmented together by the same 2 radiologists. The lesion volumes at different sites were automatically measured by computer, and the percentage of lesion extent was calculated according to lung volumes.

Vessel segmentation and quantification

Automatic segmentation of pulmonary vessels on HRCT was performed with an automated integrated segmentation method according to our previously reported method (11). Vessel parameters measured included total pulmonary vessel volume (TPVV), pulmonary vein volume (PVV), pulmonary artery volume (PAV), and the number of vessels (*Figure 2*). The following steps were performed: (I) recognition of intrapulmonary vessels by means of a computational differential geometry scheme; (II) skeletonization of intrapulmonary vessels to aid in the tracing of adjacent vessel branches; (III) the intrapulmonary vascular skeleton was traced to distinguish arteries and veins originating from extrapulmonary arteries and veins; (IV) the automatic segmentation results were checked and manually corrected by the radiologist.

Pulmonary function testing

All patients underwent PFTs and HRCT during the same week. Parameters for the study included percentage of predicted vital capacity (VC%), percentage of predicted forced vital capacity (FVC%), percentage of predicted forced expiratory volume in 1 second (FEV1%), percentage of predicted total lung capacity (TLC%), and percentage of predicted diffusing lung capacity for carbon monoxide (DLco%). In this study, patients with a 10% absolute decrease in FVC% or 15% absolute decrease in DLco% were classified as showing disease progression, otherwise they were classified as functional stability according to the ATS/ERS/JRS/ALAT 2011 guideline (1).

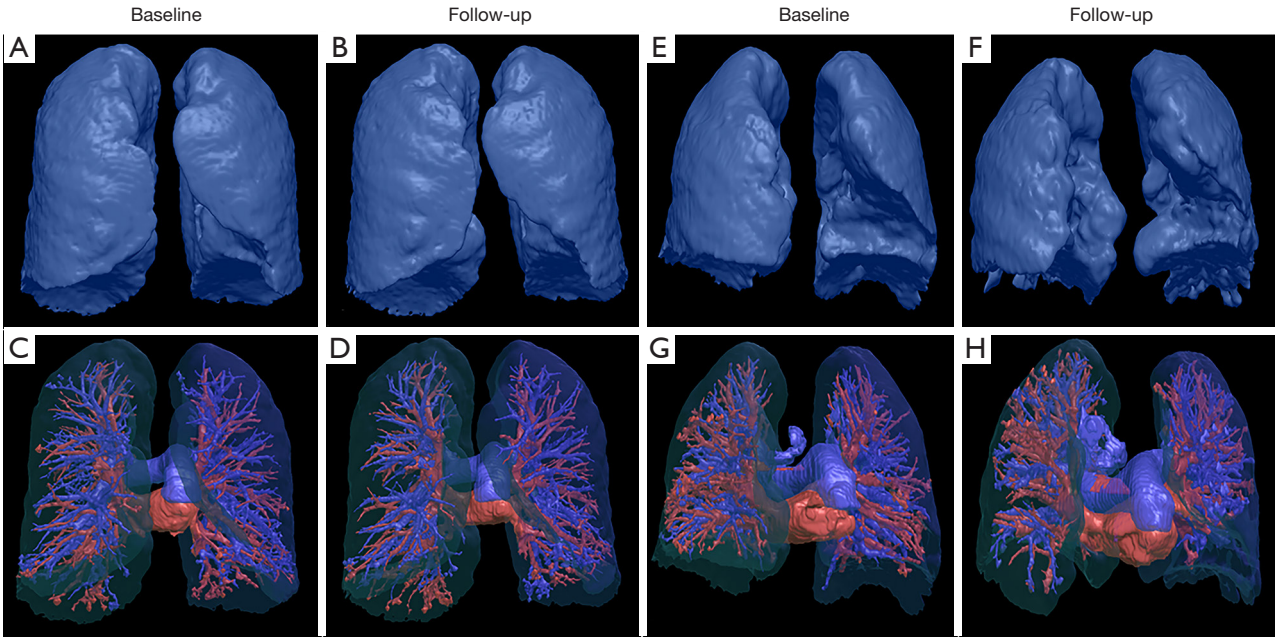

Figure 2 Chest HRCT reconstructions of changes in vessel-related parameters during the follow-up. A 61-year-old patient diagnosed with IPF demonstrated stable disease after three years of follow-up. The follow-up HRCT showed no significant changes in lung volumes (A,B) and pulmonary vessels (C,D) compared with baseline. A 67-year-old patient diagnosed with IPF demonstrated progressive disease after two years of follow-up. The follow-up HRCT showed a significant decline in lung volume (E,F) and a significant reduced number of pulmonary vessel branches (G,H) in the predominantly left lower lung compared with baseline. HRCT, high-resolution computed tomography; IPF, idiopathic pulmonary fibrosis.

Statistical analysis

All data were analyzed with SPSS 26.0 software (IBM Corp., Armonk, NY, USA). Differences between groups in the study population were compared with Student's *t*-test for quantitative data or the chi-squared test for categorical variables. Correlations between the indicators including pulmonary vessel-related parameters, pulmonary lesion extent, and PFTs were analyzed using Pearson/Spearman Rho correlation coefficients. P values were 2-tailed, and results with P<0.05 were considered statistically significant.

Results

Demographics

A total of 123 eligible patients with IPF diagnosed at the China-Japan Friendship Hospital between 2016 and 2021 were included in this study. Patients were divided into 2 groups based on PFTs: those with functional stability (n=84) and those with functional worsening (n=39). The median age of the total population was 62 years [interquartile range (IQR), 59 to 68 years] and the majority (87.0%) of patients were male (n=107). The median body mass index (BMI) was 24.6 kg/m^2 (IQR, 23.4 to 26.3 kg/m^2).

In the total population, the median baseline FVC% was 87.1% (IQR, 74.5% to 97.2%) and 43.1% of patients (n=53) showed a decrease in FVC% (<80% of the predicted value). Meanwhile, the median DLco% was 56.2% (IQR, 46.4% to 68.6%), and 78.0% of patients (n=96) exhibited a decrease in DLco% (<70% of the predicted value). There were no statistically significant differences in baseline PFTs, including VC%, FVC%, TLC%, and DLco%, between the 2 groups (with P values ranging from 0.406 to 0.839) (*Table 1*). Additionally, the median FVC% and DLco% decreased more significantly in those with functional worsening compared with those with functional stability according to the ATS/ERS/JRS/ALAT 2011 criteria [FVC%, −20.0% (IQR, −25.1% to −11.9%) *vs.* −2.4% (IQR, −5.3% to 3.1%), respectively, P<0.001; and DLco%, −18.6% (IQR, −22.5% to −13.9%) *vs.* 0.7% (−4.6% to 6.4%), respectively, P<0.001] (*Table 1*).

Table 1 Demographic and pulmonary function characteristics of patients who underwent functional assessments

Characteristics	Total patients (n=123)	Patients with functional stability (n=84)	Patients with functional worsening (n=39)	P value
Median age (years)*	62 (59 to 68)	62 (59 to 68)	63 (56 to 68)	0.854
Male, n (%)	107 (87.0)	75 (89.3)	32 (82.1)	0.267
BMI (kg/m^2)	24.6 (23.4 to 26.3)	25.4 (23.6 to 28.4)	24.0 (22.6 to 24.9)	0.002
Median baseline pulmonary function test results*				
VC%	85.4 (74.2 to 93.5)	85.6 (72.0 to 94.0)	80.5 (74.9 to 90.8)	0.802
TLC%	70.0 (62.2 to 79.5)	72.3 (59.7 to 79.7)	66.9 (63.7 to 77.9)	0.839
FVC%	87.1 (74.5 to 97.2)	86.7 (74.1 to 97.7)	89.8 (74.9 to 93.6)	0.673
DLco%	56.2 (46.4 to 68.6)	56.2 (46.2 to 67.8)	57.5 (46.4 to 69.3)	0.406
Median time intervals between baseline and follow-up CT (months)*	10.0 (4.6 to 24.3)	8.2 (3.8 to 20.2)	20.6 (8.3 to 24.8)	0.004
Median changes of pulmonary function test results*				
VC%	−4.6 (−8.2 to 2.1)	−2.3 (−5.1 to 2.7)	−13.5 (−25.6 to −12.3)	<0.001
TLC%	−1.2 (−5.2 to 3.8)	2.0 (−2.1 to 7.6)	−8.8 (−17.9 to −4.3)	<0.001
FVC%	−5.0 (−11.8 to 2.4)	−2.4 (−5.3 to 3.1)	−20.0 (−25.1 to −11.9)	<0.001
DLco%	−4.4 (−13.9 to 2.5)	0.7 (−4.6 to 6.4)	−18.6 (−22.5 to −13.9)	<0.001

*, numbers in parentheses represent the interquartile range. BMI, body mass index; VC%, percentage of predicted vital capacity; TLC%, percentage of predicted total lung capacity; FVC%, percentage of predicted forced vital capacity; DLco%, percentage of predicted diffusing lung capacity for carbon monoxide.

Quantitative analysis of different lesion sites

There were no statistically significant differences in baseline median lung volume and total lesion volume between patients with functional stability and functional worsening (P>0.05).

The median lesion volume ratio in the right lower lung was significantly higher than that in the right middle and right upper lungs at 27.50% (IQR, 15.58% to 46.17%), 6.61% (IQR, 3.80% to 13.36%), and 3.81% (IQR, 0.99% to 14.20%), respectively. The same phenomenon was observed on the left lung (*Table 2*). Additionally, there were significant negative correlations between the baseline total lesion volume ratio and the ratio of lesions at different sites (including right upper, right middle, right lower, left upper, left middle, and left lower lung) with DLco% (with R ranging from −0.66 to −0.46, P<0.001) (Table S1).

During follow-up, a significantly greater reduction in median total lung volume was observed in patients with functional worsening than in patients with functional stability [−278.01 mL (IQR, −901.64 to −91.54 mL) *vs.* −40.76 mL (IQR, −212.45 to 286.86 mL), P<0.001] and the median total lesion volume ratio increased significantly [9.38% (IQR, 2.47% to 14.0%) *vs.* −0.13% (IQR, −2.03% to 3.24%), P<0.001] (*Table 3* and *Figure 3A-3C*). Among different lesion sites, the changes in median lesion volume in the right upper lungs and right middle lungs increased more significantly for patients with functional worsening than those with functional stability. Along the same lines, median changes of lesion ratios in the right upper and right middle lungs were significantly different between the 2 groups [right upper lung, 5.40% (IQR, 0.30% to 21.02%) *vs.* 0.07% (IQR, −1.50% to 2.0%), P<0.001; right middle lung, 3.84% (IQR, 1.88% to 11.65%) *vs.* −0.07% (IQR, −2.86% to 2.47%), P<0.001], with similar results observed in the left upper and left middle lungs. However, in the left lower lungs, the differences were not statistically significant (P=0.364), although the extent of lesions increased markedly in the group with progressive disease compared with the stable group (*Table 3* and *Figure 3D-3I*). Moreover, baseline total lesion volume ratio was negatively correlated with DLco% (R=−0.66, P<0.001) (Table S1). In addition, changes in total lesion volume ratio were

Table 2 Median baseline lung volume and extent of lesions with different types and different sites based on functional assessment

Characteristics	Total patients (n=123)	Patients with functional stability (n=84)	Patients with functional worsening (n=39)	P value
Total lung volume (mL)	3,808.23 (3,414.65 to 4,606.59)	3,770.14 (3,359.05 to 4,587.80)	4,148.06 (3,531.61 to 4,993.88)	0.304
Total lesion volume (mL)	479.25 (226.98 to 764.31)	496.05 (255.94 to 757.45)	455.23 (211.98 to 856.28)	0.894
Total lesion volume ratio (%)	12.06 (6.15 to 19.12)	11.05 (6.56 to 18.94)	13.79 (5.30 to 21.38)	0.676
Extent of lesions at different sites				
Right upper lung lesion volume (mL)	23.13 (4.57 to 65.38)	20.76 (4.49 to 83.21)	26.16 (5.20 to 55.87)	0.183
Right upper lung lesion volume ratio (%)	3.81 (0.99 to 14.20)	3.53 (0.90 to 14.79)	4.65 (0.99 to 14.20)	0.243
Right middle lung lesion volume (mL)	73.72 (39.55 to 152.51)	87.76 (45.87 to 177.35)	73.72 (27.57 to 93.67)	0.107
Right middle lung lesion volume ratio (%)	6.61 (3.80 to 13.36)	7.03 (4.32 to 17.24)	6.45 (2.01 to 10.0)	0.079
Right lower lung lesion volume (mL)	116.05 (67.41 to 189.82)	112.41 (75.85 to 186.23)	137.65 (65.35 to 230.35)	0.380
Right lower lung lesion volume ratio (%)	27.50 (15.58 to 46.17)	29.41 (13.53 to 49.86)	27.49 (16.22 to 43.73)	0.555
Left upper lung lesion volume (mL)	10.59 (4.12 to 28.36)	10.93 (4.05 to 34.53)	7.78 (4.12 to 28.36)	0.140
Left upper lung lesion volume ratio (%)	2.40 (0.57 to 4.71)	2.43 (0.75 to 5.84)	1.84 (0.51 to 4.71)	0.146
Left middle lunge lesion volume (mL)	67.80 (22.98 to 121.69)	70.91 (31.09 to 118.98)	55.75 (17.77 to 146.28)	0.694
Left middle lunge lesion volume ratio (%)	7.78 (2.98 to 15.90)	7.96 (3.07 to 16.32)	5.08 (2.78 to 15.53)	0.453
Left lower lung lesion volume (mL)	88.61 (34.39 to 181.51)	88.22 (27.64 to 159.95)	153.58 (44.66 to 199.57)	0.057
Left lower lung lesion volume ratio (%)	29.79 (9.39 to 46.50)	29.09 (5.54 to 46.07)	41.17 (12.54 to 49.43)	0.217

Numbers in parentheses represent the interquartile range.

Table 3 Median changes in lung volume, extent of lesions with different types, and different sites based on functional assessments

Characteristics	Total patients (n=123)	Patients with functional stability (n=84)	Patients with functional worsening (n=39)	P value
Total lung volume (mL)	−91.54 (−457.20 to 118.44)	−40.76 (−212.45 to 286.86)	−278.01 (−901.64 to −91.54)	<0.001
Total lesion volume (mL)	50.78 (−33.17 to 169.36)	3.67 (−71.70 to 85.33)	214.73 (68.26 to 501.46)	0.001
Total lesion volume ratio (%)	1.83 (−1.35 to 8.28)	−0.13 (−2.03 to 3.24)	9.38 (2.47 to 14.0)	<0.001
Extent of lesions at different sites				
Right upper lung lesion volume (mL)	3.94 (−1.24 to 10.91)	1.17 (−5.60 to 7.11)	17.30 (2.14 to 71.43)	0.004
Right upper lung lesion volume ratio (%)	0.46 (−0.20 to 2.86)	0.07 (−1.50 to 2.00)	5.40 (0.30 to 21.02)	<0.001
Right middle lung lesion volume (mL)	6.90 (−11.09 to 42.25)	1.11 (−32.03 to 19.33)	43.32 (11.22 to 101.57)	<0.001
Right middle lung lesion volume ratio (%)	0.78(−1.69 to 4.36)	−0.07 (−2.86 to 2.47)	3.84 (1.88 to 11.65)	<0.001
Right lower lung lesion volume (mL)	13.99 (−6.41 to 30.18)	13.94 (−8.64 to 29.48)	13.99 (4.77 to 54.41)	0.174
Right lower lung lesion volume ratio (%)	1.80 (−1.40 to 8.69)	1.44 (−2.58 to 7.17)	6.34 (−0.29 to 25.97)	0.004
Left upper lung lesion volume (mL)	3.33 (−1.58 to 12.66)	0 (−6.96 to 8.06)	12.41 (3.11 to 27.53)	0.026
Left upper lung lesion volume ratio (%)	0.69 (−0.32 to 3.65)	0.06 (−1.23 to 1.10)	3.44 (1.09 to 8.19)	<0.001
Left middle lunge lesion (mL)	6.84 (−15.69 to 30.54)	−0.08 (−16.28 to 19.95)	18.66 (−6.71 to 64.20)	0.113
Left middle lunge lesion volume ratio (%)	0.88 (−1.77 to 4.42)	0.31 (−2.40 to 2.73)	4.41 (0.36 to 7.95)	0.007
Left lower lung lesion volume (mL)	2.22 (−18.28 to 43.60)	−0.14 (−17.39 to 26.93)	6.62 (−26.68 to 83.29)	0.858
Left lower lung lesion volume ratio (%)	1.72 (−1.93 to 13.73)	1.58 (−2.96 to 7.32)	4.28 (−1.31 to 35.92)	0.364

Numbers in parentheses represent the interquartile range.

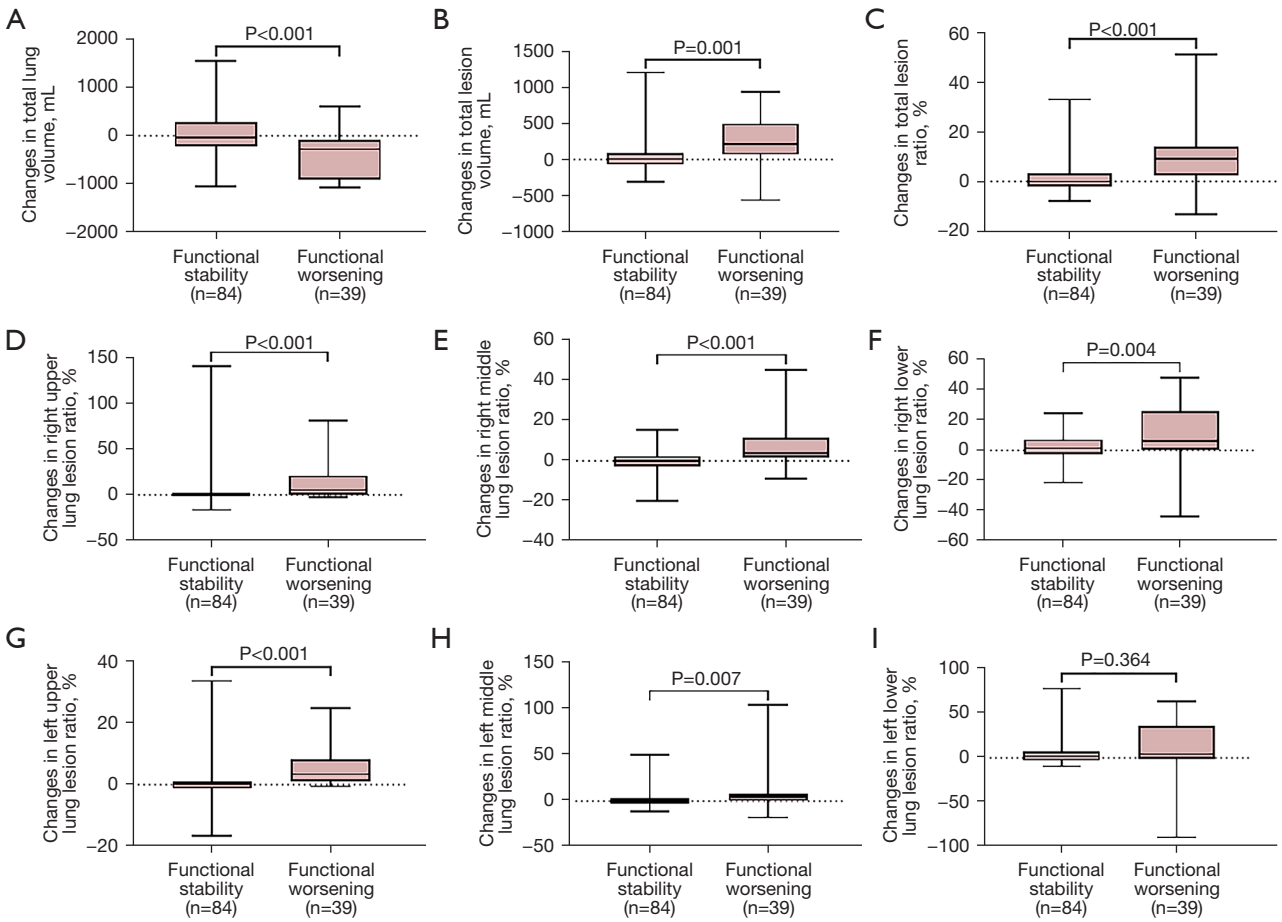

Figure 3 Differences in changes of volume of lung and lesions at different sites between groups according to functional assessment. (A) total lung volume (mL); (B) total lesion volume (mL); (C) total lesion volume ratio (%); (D) right upper lung lesion volume ratio (%); (E) right middle lung lesion volume ratio (%); (F) right lower lung lesion volume ratio (%); (G) left upper lung lesion volume ratio (%); (H) left middle lunge lesion volume ratio (%); and (I) left lower lung lesion volume ratio (%).

negatively correlated with changes in DLco% during follow-up (R=–0.57, P<0.001) (Table S2).

Quantitative analysis of vessel-related parameters

No statistically significant differences were observed between the 2 patient groups for any of the baseline vascular indicators (with P values ranging from 0.066 to 0.964) (*Table 4*). Nevertheless, baseline pulmonary vessel-related parameters were significantly correlated with DLco% (with R ranging from 0.26 to 0.39, P<0.001) (Table S1). However, TPVV, TPVV ratio, PVV, and PVV ratio, and the number of pulmonary vessel branches were found to decrease significantly in patients with disease progression compared with those with disease stability [TPVV, –28.82 mL (IQR, –43.56 to –22.79 mL) *vs.* –2.41 mL (IQR, –8.14 to 5.57 mL), respectively, P<0.001; TPVV ratio, –0.67% (IQR, –1.08% to –0.27%) *vs.* –0.03% (IQR, –0.23% to 0.12%), respectively, P<0.001; and the number of pulmonary vessel branches, –116 (IQR, –178 to –103) *vs.* –32 (IQR, –79 to 20.5), respectively, P<0.001] (*Table 4* and *Figure 4*). Meanwhile, changes in pulmonary vessel-related parameters demonstrated a statistically positive correlation with DLco% (with R ranging from 0.27 to 0.53, P<0.001) and FVC% (with R ranging from 0.44 to 0.61, P<0.001) (Table S2).

Discussion

Visual, semiquantitative parenchymal abnormality scores

Table 4 Pulmonary vascular parameters based on functional assessments

Characteristics	All patients (n=123)	Patients with functional stability (n=84)	Patients with functional worsening (n=39)	P value
Median baseline pulmonary vessel-related indexes				
TPVV (mL)	91.50 (70.84 to 108.59)	92.05 (68.64 to 107.35)	91.50 (73.22 to 110.81)	0.241
TPVV (%)	2.34 (1.97 to 2.72)	2.25 (1.90 to 2.75)	2.41 (2.21 to 2.67)	0.340
Number of pulmonary vessel branches	442 (358 to 489)	436.50 (355.75 to 479.50)	454 (362 to 516)	0.566
PAV (mL)	48.62 (37.39 to 55.35)	48.57 (37.07 to 58.15)	48.67 (37.79 to 53.30)	0.964
PAV (%)	1.25 (1.07 to 1.40)	1.26 (1.04 to 1.43)	1.19 (1.09 to 1.32)	0.752
Number of pulmonary artery branches	244 (205 to 266)	244 (202 to 269.5)	244 (210 to 258)	0.327
PVV (mL)	42.12 (32.14 to 55.01)	41.00 (31.82 to 53.25)	43.23 (32.41 to 59.08)	0.067
PVV (%)	1.13 (0.88 to 1.33)	1.06 (0.84 to 1.33)	1.18 (1.10 to 1.33)	0.066
The number of pulmonary vein branches	193 (147 to 234)	185.5 (146 to 223)	196 (152 to 256)	0.077
Median changes in pulmonary vascular indexes				
TPVV (mL)	−5.84 (−23.85 to 2.11)	−2.41 (−8.14 to 5.57)	−28.82 (−43.56 to −22.79)	<0.001
TPVV (%)	−0.17 (−0.50 to 0.11)	−0.03 (−0.23 to 0.12)	−0.67(−1.08 to −0.27)	<0.001
Number of pulmonary vessel branches	−52 (−109 to 16)	−32 (−79 to 20.5)	−116 (−178 to −103)	<0.001
PAV (mL)	−2.16 (−9.08 to 2.79)	0.81 (−3.54 to 3.27)	−11.57 (−20.27 to −8.24)	<0.001
PAV (%)	−0.04 (−0.20 to 0.07)	0.01 (−0.07 to 0.08)	−0.28 (−0.37 to −0.10)	<0.001
Number of pulmonary artery branches	−24 (−54 to −1)	−14.5 (−34.75 to −1)	−49 (−71 to −27)	0.022
PVV (mL)	−4.32 (−15.18 to 0.81)	−2.01 (−5.42 to 2.05)	−17.37 (−22.93 to −12.43)	<0.001
PVV (%)	−0.12 (−0.38 to 0.05)	−0.06 (−0.14 to 0.09)	−0.42(−0.73 to −0.17)	<0.001
Number of pulmonary vein branches	−27 (−78 to 13)	−0.5 (−45.5 to 18)	−81 (−102 to −55)	<0.001

Numbers in parentheses represent the interquartile range. TPVV, total pulmonary vessel volume; PAV, pulmonary artery volume; PVV, pulmonary vein volume.

have been reported in several studies to predict the prognosis of patients with IPF (6,12-14). Nevertheless, the reproducibility of semiquantitative scores is poor and is often limited by interobserver variability (15). The quest for sensitive, reproducible, and objective indicators for accurate assessment of disease progression has therefore received widespread attention (16-18).

HRCT is an essential imaging tool for the diagnosis and follow-up of IPF. PFTs (including FVC and DLco) represent the traditional method of determining disease severity and prognosis (1). This study provides a dynamic quantitative analysis of the extent of lesions and vessel-related parameters on chest CT in patients with IPF. Multiple studies have demonstrated the correlation of quantitative CT-based lesion extent with lung function parameters and, the utility of QCT for determining prognosis in patients with IPF (6,14,19-21). Our research reiterates this, having demonstrated that baseline lesion volume and ratio were negatively correlated with FVC% and DLco% (P<0.001). The same findings were reported for changes in lesion volumes during follow-up. A recent study by Humphries *et al.* (7) that involved baseline data-driven texture analysis showed that fibrosis scores were significantly associated with annual rates of decline in FVC and DLco. They found that higher fibrosis scores were associated with a poorer prognosis (P<0.001).

Due to a lack of adequate follow-up time, disease progression was assessed in the current study, but not survival outcomes. We found significant differences of lesion extent as well as vascular parameters (pulmonary vessel volume, number of pulmonary vessel branches) over time between the 2 patient groups, whilst there were no

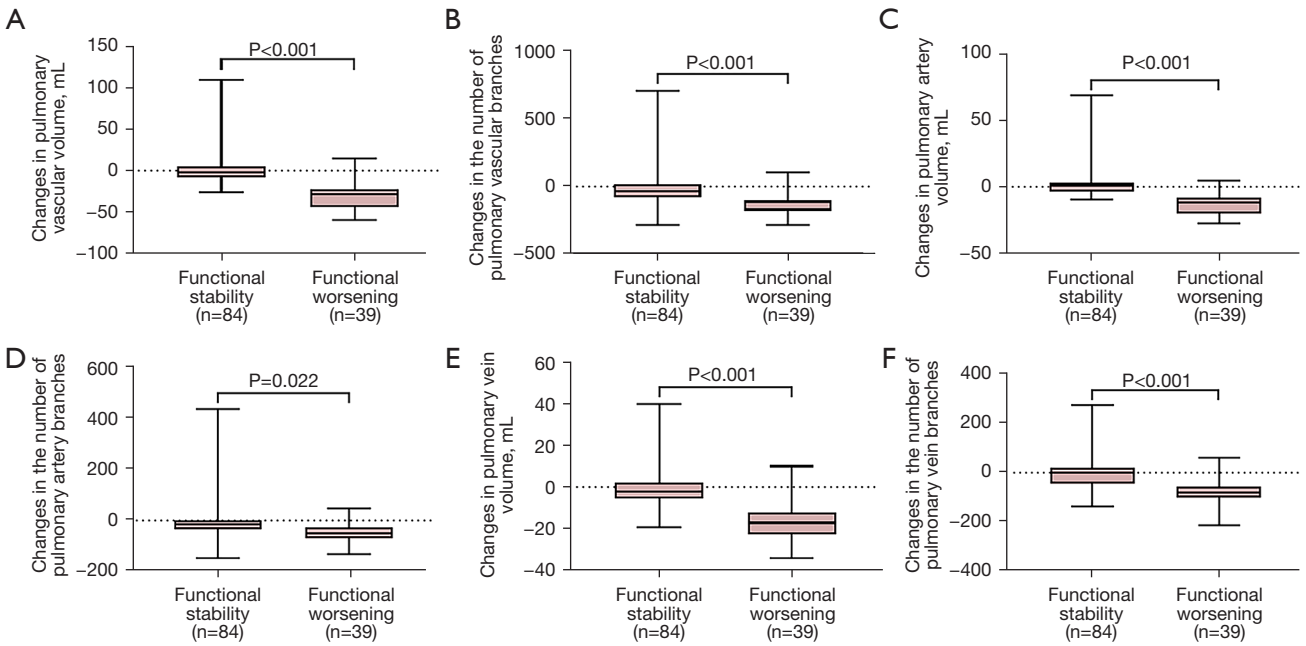

Figure 4 Differences in changes of vessel-related parameters between groups according to functional assessment. (A) TPVV; (B) the number of pulmonary vessel branches; (C) PAV; (D) the number of pulmonary artery branches; (E) PVV; and (F) the number of pulmonary vein branches. TPVV, total pulmonary vessel volume; PAV, pulmonary artery volume; PVV, pulmonary vein volume.

statistically significant differences between the 2 groups for these parameters at baseline. This, therefore, suggests that dynamic changes in these imaging findings over time are more reflective of disease severity and prognosis in IPF than findings at baseline.

Several recent studies have demonstrated the potential role of quantitative analysis of vessel-related indicators in the assessment of ILD severity and prognosis (6,10,22,23). In these studies, baseline TPVV, TPVV ratio, and the number of pulmonary vessel branches were not found to be statistically different between groups with functional stability and functional worsening. However, the current study found that changes in these indicators during follow-up were significantly different between these groups. Moreover, baseline pulmonary vessel-related parameters were significantly correlated with DLco% (with R ranging from 0.26 to 0.39, P<0.001). Interestingly, there were stronger correlations between the changes recorded in pulmonary vessel-related parameters and changes in DLco% (with R ranging from 0.27 to 0.53, P<0.001) than with baseline parameters, which further supports the predictive value of dynamic imaging indicators for disease progression and prognosis in IPF.

There are several limitations in this study. Firstly, patients with more severe disease who were unable to complete PFT were excluded from our analysis, which may have led to selection bias. Secondly, many patients failed to complete follow-up because of the impact of the coronavirus disease of 2019 (COVID-19) pandemic, thereby limiting our sample size. Finally, in cases of severe fibrosis, segmentation of pulmonary vessels is susceptible to reticular pattern contamination, which may have mitigated the relationship between pulmonary vessel-related parameters and PFTs.

Conclusions

Our study demonstrates that changes in lung lesion extent and pulmonary vessel-related parameters are significantly different between patients with IPF who display functional stability or functional deterioration according to serial PFTs. Enlargement of pulmonary lesions and reductions in pulmonary vessel volume on CT were the strongest indicators of declining FVC% and DLco%. Therefore, for patients with complete follow-up information and with high-quality chest HRCT, these imaging findings may serve as valuable indicators of disease severity and prognosis in

patients with IPF.

Acknowledgments

Funding: This work was supported by the National Key R&D Program of China (Nos. 2021YFC2500700 and 2016YFC0901101 to H Dai).

Footnote

Reporting Checklist: The authors have completed the STROBE reporting checklist. Available at https://qims.amegroups.com/article/view/10.21037/qims-22-843/rc

Conflicts of Interest: All authors have completed the ICMJE uniform disclosure form (available at https://qims.amegroups.com/article/view/10.21037/qims-22-843/coif). HK and RZ are staff of Infervision Medical Technology Co., Ltd. The school/hospital and the company are in a collaborative relationship. The other authors have no conflicts of interest to declare.

Ethical Statement: The authors are accountable for all aspects of the work in ensuring that questions related to the accuracy or integrity of any part of the work are appropriately investigated and resolved. The study was conducted in accordance with the Declaration of Helsinki (as revised in 2013). The study was approved by the Ethics Board of China-Japan Friendship Hospital (No. 2017-25), and individual consent for this retrospective analysis was waived.

References

1. Raghu G, Collard HR, Egan JJ, Martinez FJ, Behr J, Brown KK, et al. An official ATS/ERS/JRS/ALAT statement: idiopathic pulmonary fibrosis: evidence-based guidelines for diagnosis and management. Am J Respir Crit Care Med 2011;183:788-824.
2. Karimi-Shah BA, Chowdhury BA. Forced vital capacity in idiopathic pulmonary fibrosis--FDA review of pirfenidone and nintedanib. N Engl J Med 2015;372:1189-91.
3. Nathan SD, Shlobin OA, Weir N, Ahmad S, Kaldjob JM, Battle E, Sheridan MJ, du Bois RM. Long-term course and prognosis of idiopathic pulmonary fibrosis in the new millennium. Chest 2011;140:221-9.
4. Travis WD, Costabel U, Hansell DM, King TE Jr, Lynch DA, Nicholson AG, et al. An official American Thoracic Society/European Respiratory Society statement: Update of the international multidisciplinary classification of the idiopathic interstitial pneumonias. Am J Respir Crit Care Med 2013;188:733-48.
5. Oda K, Ishimoto H, Yatera K, Naito K, Ogoshi T, Yamasaki K, Imanaga T, Tsuda T, Nakao H, Kawanami T, Mukae H. High-resolution CT scoring system-based grading scale predicts the clinical outcomes in patients with idiopathic pulmonary fibrosis. Respir Res 2014;15:10.
6. Jacob J, Bartholmai BJ, Rajagopalan S, Kokosi M, Nair A, Karwoski R, Walsh SL, Wells AU, Hansell DM. Mortality prediction in idiopathic pulmonary fibrosis: evaluation of computer-based CT analysis with conventional severity measures. Eur Respir J 2017;49:1601011.
7. Humphries SM, Mackintosh JA, Jo HE, Walsh SLF, Silva M, Calandriello L, Chapman S, Ellis S, Glaspole I, Goh N, Grainge C, Hopkins PMA, Keir GJ, Moodley Y, Reynolds PN, Walters EH, Baraghoshi D, Wells AU, Lynch DA, Corte TJ. Quantitative computed tomography predicts outcomes in idiopathic pulmonary fibrosis. Respirology 2022;27:1045-53.
8. Watadani T, Sakai F, Johkoh T, Noma S, Akira M, Fujimoto K, Bankier AA, Lee KS, Müller NL, Song JW, Park JS, Lynch DA, Hansell DM, Remy-Jardin M, Franquet T, Sugiyama Y. Interobserver variability in the CT assessment of honeycombing in the lungs. Radiology 2013;266:936-44.
9. Romei C, Tavanti LM, Taliani A, De Liperi A, Karwoski R, Celi A, Palla A, Bartholmai BJ, Falaschi F. Automated Computed Tomography analysis in the assessment of Idiopathic Pulmonary Fibrosis severity and progression. Eur J Radiol 2020;124:108852.
10. Jacob J, Pienn M, Payer C, Urschler M, Kokosi M, Devaraj A, Wells AU, Olschewski H. Quantitative CT-derived vessel metrics in idiopathic pulmonary fibrosis: A structure-function study. Respirology 2019;24:445-52.

11. Sun X, Meng X, Zhang P, Wang L, Ren Y, Xu G, Yang T, Liu M. Quantification of pulmonary vessel volumes on low-dose computed tomography in a healthy male Chinese population: the effects of aging and smoking. Quant Imaging Med Surg 2022;12:406-16.
12. Jacob J, Bartholmai BJ, Rajagopalan S, Kokosi M, Egashira R, Brun AL, Nair A, Walsh SLF, Karwoski R, Wells AU. Serial automated quantitative CT analysis in idiopathic pulmonary fibrosis: functional correlations and comparison with changes in visual CT scores. Eur Radiol 2018;28:1318-27.
13. Jacob J, Aksman L, Mogulkoc N, Procter AJ, Gholipour B, Cross G, et al. Serial CT analysis in idiopathic pulmonary fibrosis: comparison of visual features that determine patient outcome. Thorax 2020;75:648-54.
14. Jacob J, Bartholmai BJ, Rajagopalan S, Kokosi M, Nair A, Karwoski R, Raghunath SM, Walsh SL, Wells AU, Hansell DM. Automated Quantitative Computed Tomography Versus Visual Computed Tomography Scoring in Idiopathic Pulmonary Fibrosis: Validation Against Pulmonary Function. J Thorac Imaging 2016;31:304-11.
15. Walsh SL, Calandriello L, Sverzellati N, Wells AU, Hansell DM; . Interobserver agreement for the ATS/ERS/JRS/ALAT criteria for a UIP pattern on CT. Thorax 2016;71:45-51.
16. Guo L, Yang Y, Liu F, Jiang C, Yang Y, Pu H, Li W, Zhong Z. Clinical Research on Prognostic Evaluation of Subjects With IPF by Peripheral Blood Biomarkers, Quantitative Imaging Characteristics and Pulmonary Function Parameters. Arch Bronconeumol (Engl Ed) 2020;56:365-72.
17. Niwamoto T, Handa T, Murase Y, Nakatsuka Y, Tanizawa K, Taguchi Y, et al. Cutaneous T-cell-attracting chemokine as a novel biomarker for predicting prognosis of idiopathic pulmonary fibrosis: a prospective observational study. Respir Res 2021;22:181.
18. Kreuter M, Lee JS, Tzouvelekis A, Oldham JM, Molyneaux PL, Weycker D, Atwood M, Kirchgaessler KU, Maher TM. Monocyte Count as a Prognostic Biomarker in Patients with Idiopathic Pulmonary Fibrosis. Am J Respir Crit Care Med 2021;204:74-81.
19. Torrisi SE, Palmucci S, Stefano A, Russo G, Torcitto AG, Falsaperla D, Gioè M, Pavone M, Vancheri A, Sambataro G, Sambataro D, Mauro LA, Grassedonio E, Basile A, Vancheri C. Assessment of survival in patients with idiopathic pulmonary fibrosis using quantitative HRCT indexes. Multidiscip Respir Med 2018;13:43.
20. Clukers J, Lanclus M, Mignot B, Van Holsbeke C, Roseman J, Porter S, Gorina E, Kouchakji E, Lipson KE, De Backer W, De Backer J. Quantitative CT analysis using functional imaging is superior in describing disease progression in idiopathic pulmonary fibrosis compared to forced vital capacity. Respir Res 2018;19:213.
21. Sun H, Liu M, Kang H, Yang X, Zhang P, Zhang R, Dai H, Wang C. Quantitative analysis of high-resolution computed tomography features of idiopathic pulmonary fibrosis: a structure-function correlation study. Quant Imaging Med Surg 2022;12:3655-65.
22. Occhipinti M, Bruni C, Camiciottoli G, Bartolucci M, Bellando-Randone S, Bassetto A, Cuomo G, Giuggioli D, Ciardi G, Fabbrizzi A, Tomassetti S, Lavorini F, Pistolesi M, Colagrande S, Matucci-Cerinic M. Quantitative analysis of pulmonary vasculature in systemic sclerosis at spirometry-gated chest CT. Ann Rheum Dis 2020;79:1210-7.
23. Puxeddu E, Cavalli F, Pezzuto G, Teodori E, Rogliani P. Impact of pulmonary vascular volume on mortality in IPF: is it time to reconsider the role of vasculature in disease pathogenesis and progression? Eur Respir J 2017;49:1602345.

Cite this article as: Sun H, Liu M, Kang H, Yang X, Zhang P, Zhang R, Dai H, Wang C. Idiopathic pulmonary fibrosis disease progression: a dynamic quantitative chest computed tomography follow-up analysis. Quant Imaging Med Surg 2023;13(3):1488-1498. doi: 10.21037/qims-22-843

